

Direct Design Approach of Discrete PI Controller for Hard Disk Drive Spindle Motors

Quan Jiang, Chao Bi, Fan Hong, Song Lin
Mechatronics & Recording Channel Division, A*Star Data Storage Institute, Singapore
E-mail: JIANG_Quan@DSI.A-Star.edu.sg

Abstract — As the area density of hard disk drives (HDD) increases, the speed of spinning media disks should be very stable. Now each HDD employs a sensorless brushless DC (BLDC) motor to spin the media platters at a constant speed. However, the drag torque of the spinning disk varies as the slider with writer and reader heads moves in or out to seek the targeted tracks, which will cause the spinning speed fluctuation. In order to reduce the amplitude of the speed fluctuation, a proportional-integral (PI) close-loop speed controller for the spindle motor should be employed. But few publications introduced the proper design of such a speed controller. This paper develops a direct approach to design the HDD spinning speed controller.

Firstly, the special features of HDD spindle motors are analyzed and a small signal equivalent model of the spindle BLDC motor is proposed based on HDD's constant spinning speed. Then a discrete PI speed controller is introduced and the design of its PI gains is studied. At last, MATLAB simulation and experimental results are presented to check the effectiveness of the proposed spindle motor model and the design methodology of the discrete PI speed controller.

I. INTRODUCTION

As hard disk drive (HDD) areal density increases, the track density and bit density increase, i.e., the track width and bit length become narrower and shorter, respectively [1, 2]. Correspondingly, the spinning speed of the spindle motor and media disk(s) should be more and more stable as the bit length becomes shorter and shorter. Now each HDD employs a sensorless brushless DC motor (BLDC) to spin the media disk(s) at a constant speed, as shown in Fig.1. But the drag torque of the spinning disk varies as the slider with writer and reader heads moves in or out to seek the targeted tracks, which causes the speed fluctuation dynamically. Also the temperature of fluid dynamic bearings (FDBs) changes and this causes the drag torque to vary slowly. In order to keep the speed constant, a proportional-integral (PI) close-loop speed control of spindle motors should be applied. But there are few publications to discuss the design of speed PI controller for HDD spindle motors. This paper will develop an approach to design the HDD spinning speed controller and its gains.

In previous publications, BLDC motors were often treated as a DC motor and the design of their speed close-loop controller simply takes the equivalent DC motor model [3, 4]. However, there are obvious differences between the DC motors and BLDC motors. For example, the commutating angle of a BLDC motor will influence the torque constant,



Fig. 1. A typical disk spinning of a hard disk drive.

which does not exist in a DC motor. The transient current waveform for a BLDC motor is alternative current, not DC current. Comparing with other kinds of BLDC motors, the HDD spindle motors need not to adjust speed but should be robust to the load variations to keep the spinning speed constant. Therefore, a more suitable model of brushless DC motors should be developed. In Section II, these special features of HDD spindle motors will be analyzed and a small signal equivalent model of the spindle BLDC motor will be developed based on HDD's constant spinning speed.

Due to the cost, space limitation and reliability requirement, all HDD spindle motors are sensorless without the rotor encoder. For a sensorless BLDC motor, only finite rotor position index moments can be obtained to detect the motor speed. So the spinning speed control has to be discrete. Correspondingly, the discrete PI control should be applied to implement the constant speed control. These will be introduced in Part C of Section II and Section III.

Through the paper, MATLAB will be employed to simulate the transient performances of the spindle motor and PI controller, including the spindle motor speed, drag torque fluctuation, phase current and phase voltage.

In Section III, the experimental results will also be introduced and compared with the simulations to verify the proposed model and design method of discrete PI speed controller.

II. MATHEMATIC MODELS OF SPINDLE MOTORS

Since HDDs are very compact in size and sensitive to the cost of the spindle motor, now all spindle motors of HDDs are sensorless three-phase permanent magnetic motors which operate in BLDC mode with sinusoidal or trapezoidal back EMFs. In this paper, a sinusoidal back EMF BLDC permanent

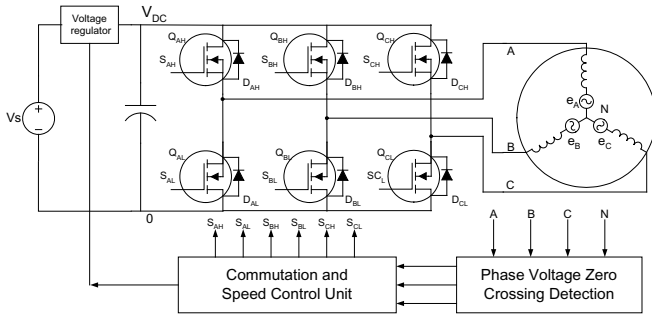


Fig. 2. A typical disk spinning of a hard disk drive.

magnet spindle motor system is instantiated, as shown in Fig. 2. In the system, an adjustable DC/DC voltage regulator is employed to realize accurate speed control in the constant voltage BLDC mode.

A. General Mathematic Model of BLDC Spindle Motors

In general, a permanent magnet (PM) motor with sinusoidal back EMF waveform can be modeled by the following equations [5]:

$$\begin{cases} e_A(\theta) = k_e p_p \omega \sin(p_p \theta) \\ e_B(\theta) = e_A(p_p \theta - \frac{2}{3}\pi) = k_e p_p \omega \sin(p_p \theta - \frac{2}{3}\pi) \\ e_C(\theta) = e_A(p_p \theta - \frac{4}{3}\pi) = k_e p_p \omega \sin(p_p \theta - \frac{4}{3}\pi) \end{cases} \quad (1)$$

$$i_A + i_B + i_C = 0 \quad (2)$$

$$\begin{bmatrix} V_A \\ V_B \\ V_C \end{bmatrix} = \begin{bmatrix} e_A \\ e_B \\ e_C \end{bmatrix} + \begin{bmatrix} R_A & & \\ & R_B & \\ & & R_C \end{bmatrix} \begin{bmatrix} i_A \\ i_B \\ i_C \end{bmatrix} + \begin{bmatrix} L_{AA} & M_{AB} & M_{AC} \\ M_{AB} & L_{BB} & M_{BC} \\ M_{AC} & M_{BC} & L_{CC} \end{bmatrix} \frac{d}{dt} \begin{bmatrix} i_A \\ i_B \\ i_C \end{bmatrix} + \begin{bmatrix} V_n \\ V_n \\ V_n \end{bmatrix} \quad (3)$$

$$T_{em} = \frac{1}{\omega} (e_A \times i_A + e_B \times i_B + e_C \times i_C) \quad (4)$$

$$J \frac{d\omega}{dt} = T_{em} + T_c - T_f - T_w \quad (5)$$

$$\omega = \frac{2\pi}{60} n = \frac{d\theta}{dt} \quad (6)$$

where V_A , V_B , and V_C are terminal voltages of the motor, V_n is the neutral point voltage, i_A , i_B and i_C are phase currents, e_A , e_B , and e_C are phase back EMFs, R_A , R_B , and R_C are phase resistances, L_{AA} , L_{BB} , and L_{CC} are phase self inductances, M_{AB} , M_{BC} and M_{AC} are phase to phase mutual inductances, p_p is the

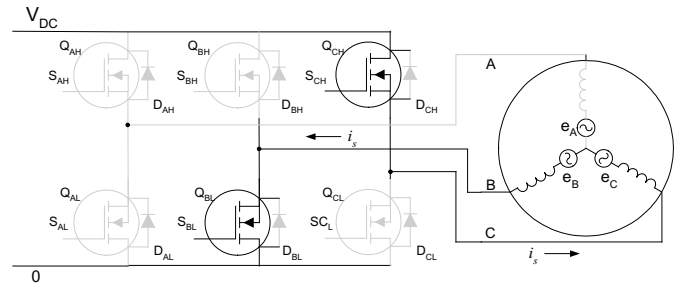


Fig. 3. Normal operating status of inverter in period 1.

number of pole-pairs, T_{em} is the electromagnetic torque produced by the phase currents, T_c is the cogging torque, J is the system inertia, ω is the mechanical angular speed, n is the corresponding speed in rpm, θ is the rotor position in mechanical radian relative to the stator, T_f is the bearing friction torque, and T_w is the windage aerodynamic drag on the HDD spinning rotor and media discs. Now the cogging torque is very small and is neglected in this paper.

When a spindle motor operates in BLDC mode with an advanced commutating electrical angle β , the switches and diodes will operate in sequence as shown in Table I. The operating periods can be classified into two categories, i.e., normal two-phase conducting periods and phase commutating periods caused by the phase inductance. In Table I, the commutating period is supposed to last $\delta_c/(p_p \omega)$ seconds.

During the period 1, when MOSFET Q_{CH} and Q_{BL} are switched on in Fig. 3, the terminal voltages and phase currents can be expressed as:

$$V_A = e_A + V_n, V_B = -i_B r_{DS}, V_C = V_{DC} - i_C r_{DS} \quad (6)$$

$$i_A = 0 \text{ and } i_B = -i_C \quad (7)$$

where r_{DS} is on-resistance of MOSFET switches. From (3), (6) and (7), the neutral point voltage is obtained as:

$$V_n = \frac{1}{2}(V_{DC} + e_A) \quad (8)$$

$$V_A = V_{DC} - r_{DS} i_A, V_B = -i_B r_{DS} \text{ and } V_C = -V_F \quad (9)$$

$$V_n = \frac{1}{3}(V_{DC} - r_{DS} i_A - r_{DS} i_B - V_F) = \frac{1}{3}(V_{DC} + r_{DS} i_C - V_F) \quad (10)$$

where V_F is the voltage drop of the MOSFET anti-parallel diode during freewheeling.

When the rotor reaches the position of $\pi/6 - \beta$, the commutation from the exciting phase C to the phase A will happen and last till the phase current i_C drops to zero, i.e., the period C_{12} in Table I, as shown in Fig. 4. During this

TABLE I
BLDC OPERATING AND COMMUTATING PERIODS

	1	C_{12}	2	C_{23}	3	C_{34}
Periods	$(-\frac{\pi}{6} - \beta + \delta_c, \frac{\pi}{6} - \beta)$	$(\frac{\pi}{6} - \beta, \frac{\pi}{6} - \beta + \delta_c)$	$(\frac{\pi}{6} - \beta + \delta_c, \frac{\pi}{2} - \beta)$	$(\frac{\pi}{2} - \beta, \frac{\pi}{2} - \beta + \delta_c)$	$(\frac{\pi}{2} - \beta + \delta_c, \frac{5\pi}{6} - \beta)$	$(\frac{5\pi}{6} - \beta, \frac{5\pi}{6} - \beta + \delta_c)$
“On”	Q_{CH}, Q_{BL}	Q_{AH}, Q_{BL}, D_{CL}	Q_{AH}, Q_{BL}	Q_{AH}, Q_{CL}, D_{BH}	Q_{AH}, Q_{CL}	Q_{BH}, Q_{CL}, D_{AL}
Periods	$(\frac{5\pi}{6} - \beta + \delta_c, \frac{7\pi}{6} - \beta)$	$(\frac{7\pi}{6} - \beta, \frac{7\pi}{6} - \beta + \delta_c)$	$(\frac{7\pi}{6} - \beta + \delta_c, \frac{3\pi}{2} - \beta)$	$(\frac{3\pi}{2} - \beta, \frac{3\pi}{2} - \beta + \delta_c)$	$(\frac{3\pi}{2} - \beta + \delta_c, \frac{11\pi}{6} - \beta)$	$(\frac{11\pi}{6} - \beta, \frac{11\pi}{6} - \beta + \delta_c)$
“On”	Q_{BH}, Q_{CL}	Q_{BH}, Q_{AL}, D_{CH}	Q_{BH}, Q_{AL}	Q_{CH}, Q_{AL}, D_{BL}	Q_{CH}, Q_{AL}	Q_{CH}, Q_{BL}, D_{AH}

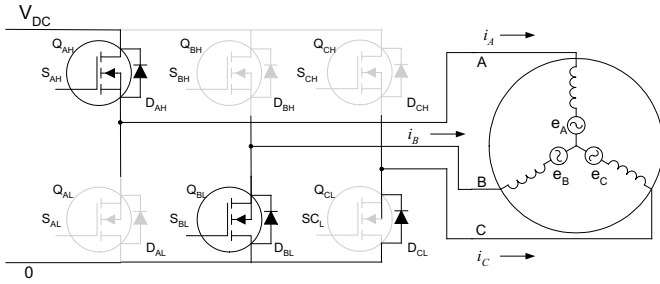


Fig. 4. Normal operating status of inverter in period C12.

commutation transient period, switches Q_{AH} and Q_{BL} as well as freewheeling diode D_{CL} are “On” and the other switches are “Off”. Then the terminal voltages and the neutral point voltage can be expressed as,

$$V_A = V_{DC} - r_{DS}i_A, V_B = -i_B r_{DS} \text{ and } V_C = -V_F \quad (9)$$

$$V_n = \frac{1}{3}(V_{DC} - r_{DS}i_A - r_{DS}i_B - V_F) = \frac{1}{3}(V_{DC} + r_{DS}i_C - V_F) \quad (10)$$

where V_F is the voltage drop of the MOSFET anti-parallel diode during freewheeling.

Through MATLAB simulation, the DC link voltage of the inverter, the BLDC motor phase voltages and currents, the electromagnetic torque and the transient speed can be easily simulated as shown in Fig. 5. In Fig. 5, the motor speed is around 15,000 rpm with the ripple of 0.017 rpm, the average electromagnetic torque is 0.004 Nm and the commutating angle is 0° (elec. deg.), the natural commutating angle of BLDC mode.

When the commutating angle β is different, the performances of the BLDC spindle motor, such as, inverter DC link voltage, phase current RMS value, input power and torque ripples, will change although the motor speed is same. Figs. 6 and 7 display other two typical operation modes with the smallest speed ripple and the least input phase RMS currents. Table II lists these three BLDC operation statuses. It is apparent that the operations of BLDC spindle motors are different from ones of DC motors.

TABLE II
SPINDLE MOTOR TYPICAL BLDC OPERATION MODES

$n = 15,000 \text{ rpm}$ and $T_{em}(\text{avg.}) = 0.004 \text{ Nm}$

β	Vdc(V)	P _{in} (W)	I _{RMS} (A)	ΔT_{pp} (Nm)	Δn_{pp} (rpm)
-3.6°	9.270	6.861	0.631	0.00183	0.0197
0°	9.315	6.865	0.634	0.00179	0.0168
4.5°	9.333	6.878	0.642	0.00169	0.0147

B. Signal Model of BLDC Spindle Motors

As introduced in Section I, HDD spindle motors need a speed close-loop controller to keep the spinning speed constant. In order to design the controller, the plant of the spindle motor should be built firstly. It is well known that HDD spindle motor normally runs at only the rated speed without the speed adjustment. The speed controller task is to control the speed constant through adjusting the DC link voltage V_{DC} of the inverter when the drag torque of spindle motor varies, which may be caused by the air windage or fluid

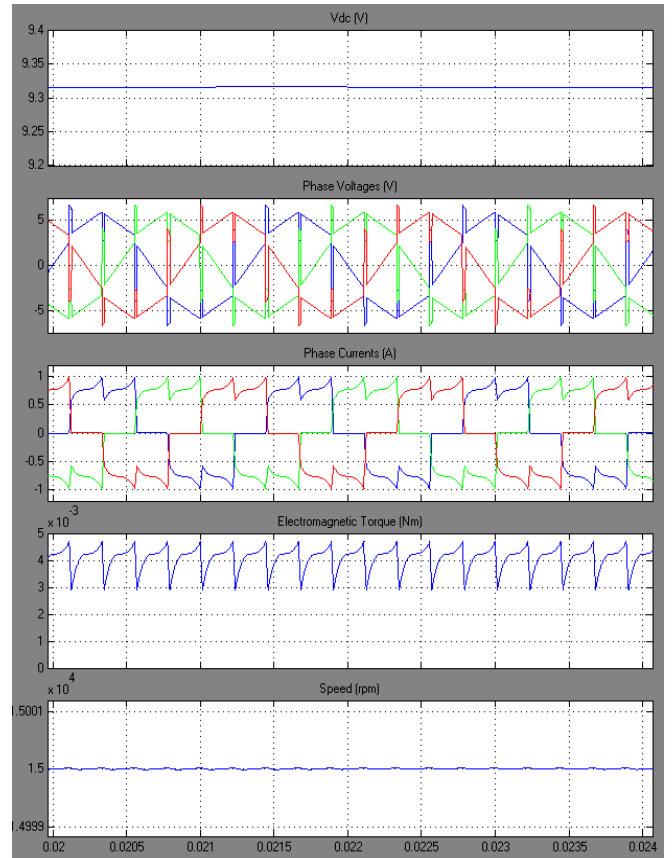


Fig. 5. Steady state operation of a spindle motor spinning at 15,000 rpm.

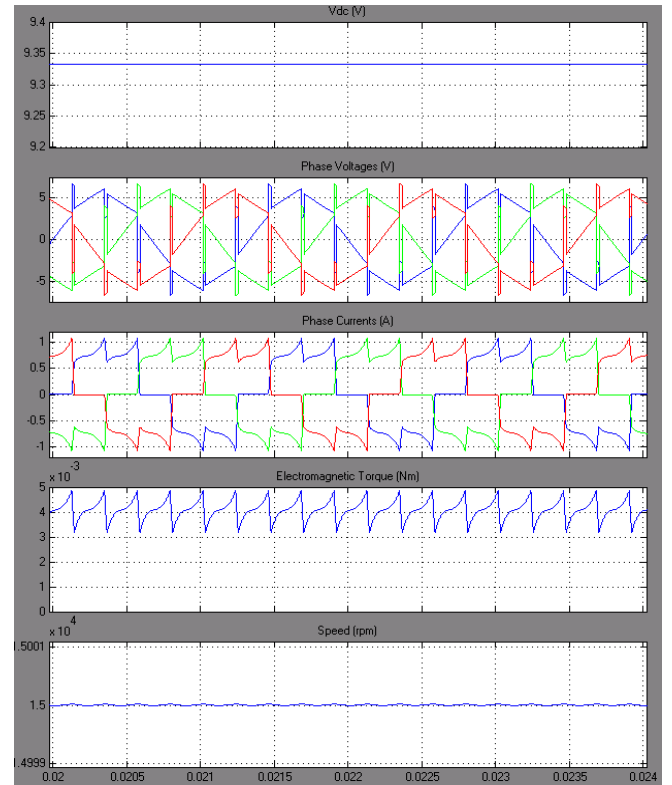


Fig. 6. Steady state operation of a spindle motor spinning at 15,000 rpm with the minimum speed ripple.

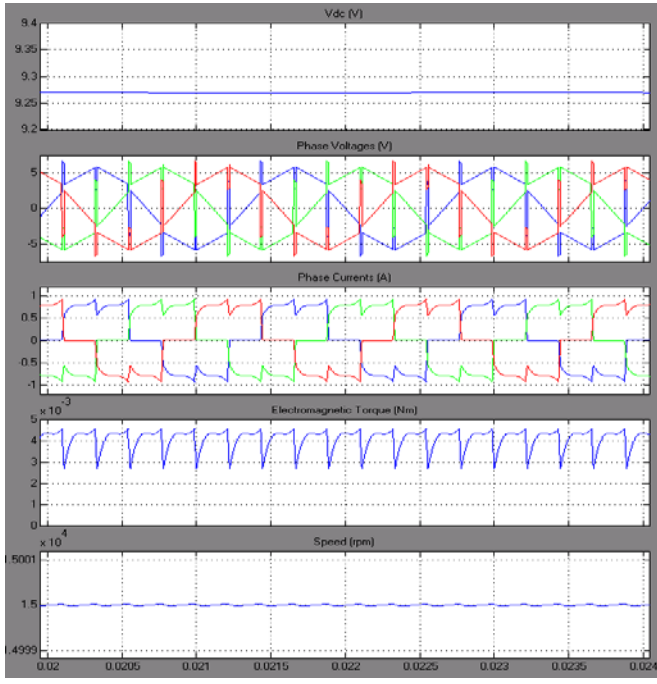


Fig. 7. Steady state operation of a spindle motor spinning at 15,000 rpm with the minimum phase RMS current and the minimum input power.

dynamic bearings. Luckily, the speed fluctuation is quite small when the drag torque changes. Therefore a small signal model of spindle motors can be developed by defining:

$$\omega(t) = \bar{\omega} + \Delta\omega(t) \text{ or } n(t) = \bar{n} + \Delta n(t) \quad (11)$$

$$V_{DC}(t) = \bar{V}_{DC} + \Delta V_{DC}(t) \quad (12)$$

$$T_{em}(t) = \bar{T}_{em} + \Delta T_{em}(t) \quad (13)$$

where $\bar{\omega}$, \bar{n} , \bar{V}_{DC} and \bar{T}_{em} are the average values during each electrical 60° , one commutating cycle in Table I, and $\Delta\omega(t)$, $\Delta n(t)$, $\Delta V_{DC}(t)$, and $\Delta T_{em}(t)$. Therefore, (5) can be simplified as:

$$J \frac{d\Delta\omega}{dt} = \Delta T_{em}(t) - \Delta T_f(t) - \Delta T_w(t) = \Delta T_{em}(t) - \Delta T_d(t) \quad (14)$$

$$\Delta T_{em}(t) = T_{em}(\bar{V}_{DC} + \Delta V_{DC}(t), \bar{\omega} + \Delta\omega(t)) - \bar{T}_{em}(\bar{V}_{DC}, \bar{\omega}) \quad (14)$$

$$\bar{T}_{em}(\bar{V}_{DC}, \bar{\omega}) = \bar{T}_f(\bar{\omega}) + \bar{T}_w(\bar{\omega})$$

$$\Delta T_d(t) = \Delta T_f(t) + \Delta T_w(t)$$

where $\Delta T_d(t)$ is the sum of the drag torque variations caused by the bearing and windage and the variation of the electromagnetic torque $\Delta T_{em}(t)$ is expressed implicitly as the function of the DC link voltage and speed.

C. Discrete Small Signal Model of a BLDC Spindle Motor

HDD spindle motors have to apply the discrete model because the control is implemented through a digital microcontroller and there is no encoder for the speed feedback detection. The possible finest control sampling time is 60° electrical degree, i.e., the commutating cycle, as shown in Figs. 5 to 7 and Table I, and it is:

$$T_s = \frac{\pi}{3p_p \bar{\omega}} = \frac{10}{p_p \bar{n}} \quad (15)$$

During the sampling period, the average electromagnetic torque can be expressed as:

$$T_{avg} = \frac{P_p}{\bar{\omega} T_s} \int_{\frac{\pi}{6p_p}}^{\frac{\pi}{2p_p}} (e_A i_A + e_B i_B + e_C i_C) d\theta \quad (16)$$

So (14) can be discretized as follows:

$$J \frac{\Delta\omega(i) - \Delta\omega(i-1)}{T_s} = \Delta T_{em}(i) - \Delta T_d(i) \quad (17)$$

$$\begin{aligned} \Delta T_{em}(i) &= T_{avg}(\bar{V}_{DC} + \Delta V_{DC}(i), \bar{\omega} + \Delta\omega(i)) - T_{avg}(\bar{V}_{DC}, \bar{\omega}) \\ &\approx \left. \frac{\partial T_{avg}(\beta)}{\partial V_{DC}} \right|_{\omega=\bar{\omega}} \Delta V_{DC}(i) + \left. \frac{\partial T_{avg}(\beta)}{\partial \omega} \right|_{V_{DC}=\bar{V}_{DC}} \Delta\omega(i) \\ &= K_v(\beta, \bar{\omega}) \Delta V_{DC}(i) + K_\omega(\beta, \bar{V}_{DC}) \Delta\omega(i) \end{aligned} \quad (18)$$

where

$$K_v(\beta, \bar{\omega}) = \left. \frac{\partial T_{avg}(\beta)}{\partial V_{DC}} \right|_{\omega=\bar{\omega}} \text{ and } K_\omega(\beta, \bar{V}_{DC}) = \left. \frac{\partial T_{avg}(\beta)}{\partial \omega} \right|_{V_{DC}=\bar{V}_{DC}} \quad (19)$$

Therefore, the discrete model of a BLDC motor can be simplified as:

$$\left[J - T_s K_\omega(\beta, \bar{V}_{DC}) \right] \Delta\omega(i) = J \Delta\omega(i-1) + T_s K_v(\beta, \bar{\omega}) \Delta V_{DC} - T_s \Delta T_d(i) \quad (20)$$

In order to obtain the coefficient $K_v(\beta, \bar{\omega})$, the steady-state BLDC operations of the spindle motor are simulated with different inverter DC link voltage V_{DC} at the same speed of 15,000 rpm. The simulation results are shown in Table III and Fig. 8. Applying the least square method (LSM), the coefficient is:

$$K_v(0^\circ, 500\pi) = 0.004 \text{ (Nm/V)} \quad (21)$$

TABLE III
SPINDLE MOTOR OPERATIONS WITH DIFFERENT VDC VALUES
 $n = 15,000 \text{ rpm}$ and $\beta = 0^\circ$

$V_{DC}(V)$	8.8	8.9	9.0	9.1	9.2
$T_{avg}(\text{mNm})$	2.037	2.430	2.822	3.223	3.619
$V_{DC}(V)$	9.3	9.4	9.5	9.6	9.7
$T_{avg}(\text{mNm})$	4.014	4.419	4.819	5.218	5.624

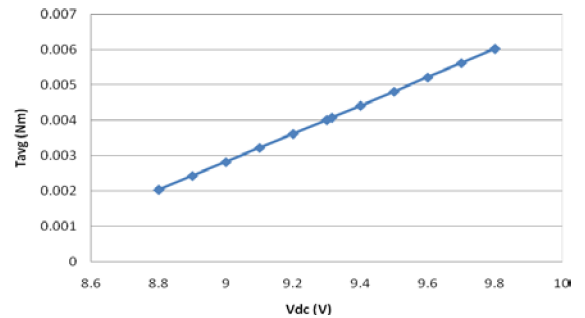


Fig. 8. Average electromagnetic torque with the different V_{DC} s.

TABLE IV
SPINDLE MOTOR OPERATIONS AT DIFFERENT SPEEDS

$V_{DC} = 9.315V$ and $\beta=0^\circ$					
$n(\text{rpm})$	14500	14600	14700	14800	14900
$T_{avg}(\text{mNm})$	5.251	5.009	4.775	4.538	4.306
$N(\text{rpm})$	15000	15100	15200	15300	15400
$T_{avg}(\text{mNm})$	4.076	3.841	3.617	3.382	3.153

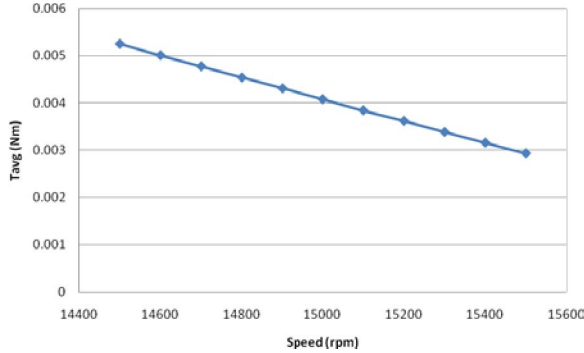


Fig. 9. Average electromagnetic torque at the different speeds.

Similarly, the average electromagnetic torque during the motor steady-state BLDC operations is simulated at the different speeds when the DC-link voltage is kept to be constant, i.e., voltage $V_{DC} = 9.315V$. It is shown in Table IV and Fig. 9. The corresponding coefficient is:

$$K_\omega(0^0, 9.315V) = -2.22 \times 10^{-5} \text{ (Nm/rad/s)} \quad (22)$$

III. DISCRETE PI CONTROLLER FOR BLDC SPINDLE MOTORS

A. PI Control and Its Gains

As mentioned above, the speed close-loop control should be used to keep the spinning speed constant when the drag torque changes. As PI control is the most mature technique, it is also used to control the spinning speed [6]. A discrete PI controller is given as follows:

$$\Delta V_{DC}(i) = -k_p \Delta \omega(i) - k_I T_s \sum_{j=1,2,3,\dots}^i \Delta \omega(j) \quad (23)$$

where k_p and k_I are the proportional and integral gains of PI controller. Fig. 10 shows the schematic of the closed-loop systems using PI control, where $\omega(k)$ is the angular speed, ω_{ref} is the reference angular speed and V_{DC} is the control signal, to maintain the speed when subject to drag torque perturbation as denoted by $T_d(i)$. The objective is to find the right values of k_p and k_I so that the closed-loop system can meet the control specifications.

The PI control is given by

$$\Delta V_{DC}(i) = -k_p \omega(i) - k_I \frac{T_s}{1-z^{-1}} \omega(i) \quad (24)$$

The closed-loop transfer function from $T_d(i)$ to $\Delta \omega(i)$ is

$$\frac{\Delta \omega(i)}{T_d(i)} = \frac{z^2 - z}{\left(\frac{J}{T_s} - K_\omega + K_v k_p + K_v k_I T_s\right) z^2 - \left(\frac{2J}{T_s} - K_\omega + K_v k_p\right) z + \frac{J}{T_s}} \quad (25)$$

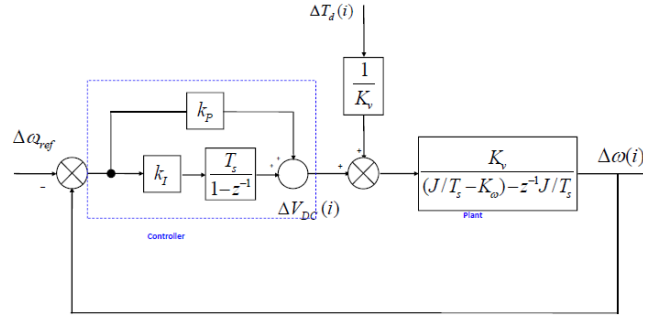


Fig. 10. Schematic of closed-loop speed control.

B. Specifications

The objective of the spindle motor speed closed-loop control is to maintain a constant steady-state reference speed in the face of drag torque perturbation. For specified values of settling time $T_{settling}$ and overshoot M_p , the requirement for damping ratio ζ and undamped natural frequency ω_n is given as:

$$\zeta \geq \zeta(M_p) = \frac{-\ln(M_p)}{\sqrt{\pi^2 + [\ln(M_p)]^2}} \quad (26)$$

$$\zeta \omega_n \geq \frac{4.6}{T_{settling}} \quad (27)$$

Based on the mapping of damping ratio and natural frequency from the s-plane to the z-plane, we have

$$\frac{\frac{2J}{T_s} - K_\omega + K_v k_p}{\frac{J}{T_s} - K_\omega + K_v k_p + K_v k_I T_s} = 2e^{-\zeta \omega_n T_s} \cos(\omega_n \sqrt{1-\zeta^2} T_s) \quad (28)$$

$$\frac{\frac{J}{T_s}}{\frac{J}{T_s} - K_\omega + K_v k_p + K_v k_I T_s} = e^{-2\zeta \omega_n T_s} \quad (29)$$

Now it is ready to obtain the relationship between k_p , k_I and ζ , ω_n as

$$k_p = \frac{\frac{2J}{T_s} e^{\zeta \omega_n T_s} \cos(\omega_n \sqrt{1-\zeta^2} T_s) - \frac{2J}{T_s} + K_\omega}{K_v} \quad (30)$$

$$k_I = \frac{\frac{J}{T_s} \left[e^{2\zeta \omega_n T_s} - 2e^{\zeta \omega_n T_s} \cos(\omega_n \sqrt{1-\zeta^2} T_s) + 1 \right]}{K_v T_s} \quad (31)$$

Since both k_p and k_I are monotonically increasing with respect to $e^{\zeta \omega_n T_s}$, the requirement of the overshoot and settling time can be transformed to

$$k_p \geq k_p(\zeta, \omega_n) \text{ and } k_I \geq k_I(\zeta, \omega_n) \quad (32)$$

For an instantiated 15,000 rpm and 3 pole-pairs spindle motor with 2 disk platters, its key parameters are as follows:

- (a) Spindle system inertia: $J = 1.72 \times 10^{-5} \text{ kgm}^2$;
- (b) Sampling time: $T_s = 0.000222 \text{ s}$;
- (c) Torque variation ratios against V_{DC} voltage and speed: $K_v = 0.004 \text{ Nm/V}$ and $K_\omega = -2.22 \times 10^{-5} \text{ Nm/rad/s}$.

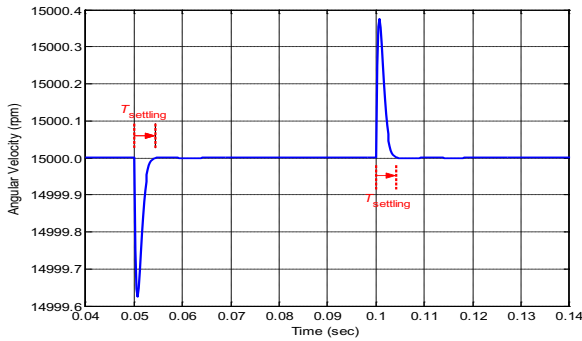


Fig. 11. Simulation results of closed-loop speed control based on discrete small signal model.

Therefore, the PI controller gains of k_p and k_i should be greater than 11.6 and 8953 respectively when the settling time $T_{settle} \leq 0.004s$ and overshoot $M_p \leq 0.01\%$ are required.

Fig. 11 shows the simulation results of the closed-loop speed control using the above gain values. It can be seen that when the system is subject to drag torque variations, the speed can be maintained with ripples of ± 0.4 rpm and 0.004s. They reach the targeted values.

Fig. 12 shows the corresponding Matlab simulation results of speed fluctuation and torque waveform based on the general mathematical model of the BLDC spindle motor when the drag torque is changed. Fig. 13 displays its experimental speed fluctuation when the drag torque is changed when the designed gains of k_p and k_i are applied.

Comparing the speed fluctuations in Figs. 11, 12 and 13, it is seen that the designed discrete PI controller with the above gains can control the speed very stably when the drag torque is changed greatly. The speed ripple is about 1 rpm, less than 0.01% of 15,000 rpm.

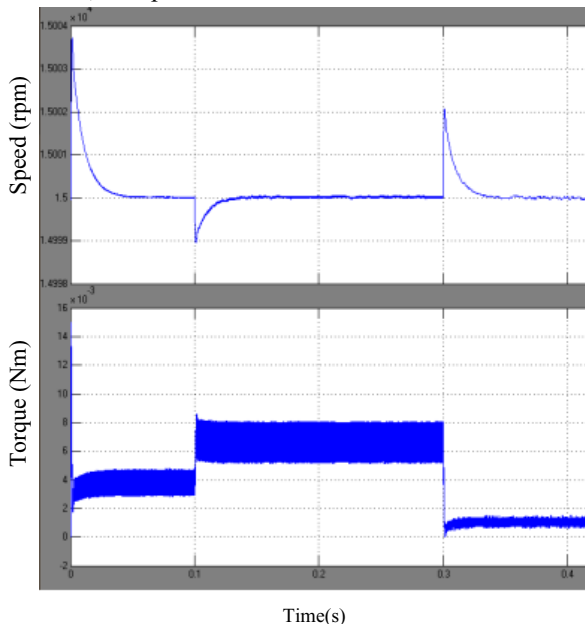


Fig. 12 Simulation results of closed-loop speed control from general model when the drag torque increases and decreases.

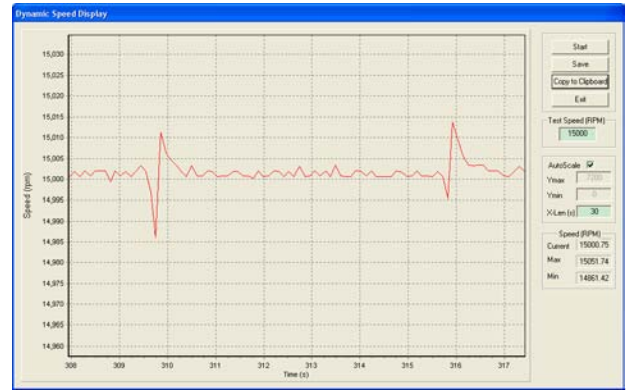


Fig. 13 Experimental speed fluctuation when the drag torque is changed.

IV. CONCLUSION

According to the special operation features of HDD spindle motors, the small signal model of a BLDC motor and the corresponding discrete small model of a sensorless BLDC motor have been developed in order to apply PI control. A discrete PI controller is employed to achieve the robust constant speed control of an HDD spindle motor. Based on the proposed discrete small signal model of the spindle motor, the direct design method of the PI controller, i.e., how to design the proportional gain k_p and integral gain k_i as well as the sampling time T_s for HDD BLDC spindle motors have been given from (30) to (32) when the specified values of settling time T_{settle} and overshoot M_p , are set. Both Matlab simulation and experiments have proven the correctness of the model of the HDD spindle motors, PI controller and its gains. The experimental results have shown that the designed controller can realize the speed ripple less than 0.01%, much better than conventional 0.1%.

The most important is that now there is a direct approach to design the discrete PI controller and its gains for HDD spindle motors. Therefore, empirical methods for tuning PI gains, such as Ziegler-Nichols rules, are not needed for HDD spindle motors. In future, the proposed method will be improved with derivative part and further developed for other kinds of BLDC motors.

REFERENCES

- [1] Y. Shiroishi, K. Fukuda, I. Tagawa, H. Iwasaki, S. Takenoiri, H. Tanaka, H. Mutoh, and N. Yoshikawa, "Future options for HDD storage", *IEEE Transactions on Magnetics.*, Vol. 45, No. 10, pp.3816-3822, Oct. 2009.
- [2] B. Marchon and T. Olson, "Magnetic Spacing Trends: From LMR to PMR and Beyond", *IEEE Transactions on Magnetics.*, Vol. 45, No. 10, pp.3608-3611, Oct 2009.
- [3] Gwo-Ruey Yu and Rey-Chue Hwang, "Optimal PID Speed Control of Brushless DC Motors Using LQR Approach", *IEEE International Conference on Systems, Man and Cybernetics*, 2004.
- [4] C.S. Soh, C. Bi, K.C. Chua, "Direct PID tuning for spindle motor systems," *Digest of Asia-Pacific Magnetic Recording Conference*, pp.P1-P2, Nov. 29-Dec. 1, 2006.
- [5] Q. Jiang and C. Bi, "An effective approach to predict performances of high speed BLDC motors in hard disk drives," *IECON'03*, Vol.3 pp.2120-2125, 2-6 Nov. 2003.
- [6] G. F. Franklin, J. D. Powell and A. Emami-Naeini, *Feedback Control of Dynamic Systems*, 4th ed., Upper Saddle River, NJ: Prentice Hall, 2002.